

The effect of sintering conditions on tailoring the magnetic properties of high permeability Mn-Zn-ferrites

J. HANUSZKIEWICZ¹, D. HOLZ¹, V. TSAKALOU², V. ZASPALIS²

¹ Ferroxcube Polska,

² Laboratory of Inorganic Materials, Center for Research and Technology-Hellas, Thessaloniki, Greece
e-mail: justyna.kalarus@ferroxcube.com

Abstract

The permeability in polycrystalline Mn-Zn-ferrites depends on a number of microstructural parameters such as grain size, porosity, structure and composition of the grain boundaries. The grain boundaries with the specific resistivity - ρ and thickness - δ , plays an important role in creating the frequency stability of the initial permeability. The sintering conditions are one of the most appropriate process by which we can influence the grain boundaries composition, specific resistivity, microstructure and magnetic properties of polycrystalline Mn-Zn-ferrites.

In this paper, it will be experimentally demonstrated, for samples with similar Mn-Zn-ferrites compositions and application of different maximum temperature of sintering, dwell time during sintering, how we may lead to the properties modification, by influencing the dopants ion diffusion and second phase segregation at the grain boundaries.

Keywords: Sintering, grain boundaries, magnetic properties, ferrites

WPŁYW WARUNKÓW SPIEKANIA NA KSZTAŁTOWANIE WŁAŚCIWOŚCI FERRYTÓW Mn-Zn O DUŻEJ PRZENIKALNOŚCI

Przenikalność polikrystalicznych ferrytów Mn-Zn zależy prócz składu chemicznego również od parametrów mikrostrukturalnych, takich jak wielkość ziarna, porowatość i charakterystyka granic ziarnowych. Granice ziarnowe z głównymi parametrami: grubością - δ i opornością właściwą - ρ , odgrywają istotną rolę w kształtowaniu nie tylko poziomu ale i stabilności częstotliwościowej przenikalności początkowej. Warunki spiekania są procesem, poprzez który możemy wpływać na skład chemiczny granic ziarnowych, oporność właściwą, mikrostrukturę i własności magnetyczne pokrystalicznych ferrytów Mn-Zn.

Praca ta demonstruje eksperymentalnie, jak poprzez zastosowanie różnych czasów przebywania materiału w maksymalnej temperaturze spiekania, możemy wpływać na modyfikację własności poprzez dyfuzję domieszek i ich segregację na granicach ziarnowych.

Słowa kluczowe: spiekanie, granice międzyziarnowe, właściwości magnetyczne, ferryty

Introduction

The permeability of polycrystalline Mn-Zn-ferrites depends, besides on the basic chemical composition also on morphological parameters such as grain size, porosity, and grain boundary characteristics. Especially the structure of the grain boundaries, with its main parameters thickness and specific resistivity, plays an important role in determining not only the level but also the frequency stability of the initial permeability. The grain boundary region is mainly differentiated from the bulk grain region because of the high concentration of structural and chemical defects. These may result either from the misfit of the crystal lattice of neighboring grains, or from the accumulation of foreign elements that do not fit to the spinel structure of ferrites. The ability to tailor the grain boundary properties is a major task that will enable the development of polycrystalline ferrite systems with better magnetic properties.

In this work the effect of sintering conditions on the grain boundary properties and through this on the magnetic behaviour of the samples is investigated. As found, the d.c.

specific resistivity of Mn-Zn-ferrites with basic composition $Mn_{0.51}Zn_{0.42}Fe_{2.06}O_4$ passes through a maximum as a function of the maximum temperature of sintering dwell time. This is in contradiction with the observed increase of the average grain. It is therefore proposed that the distribution of dopants in the microstructure varies during sintering and under circumstances may determine the specific resistivity of the microstructure and through this the magnetic behavior of the polycrystalline specimens.

Experimental

Toroidally shaped specimens (inside diameter = 18 mm, outside diameter = 30 mm, height = 14 mm) are produced by uniaxial compaction of spray dried granules with the chemical compositions (as determined by X-ray fluorescence) shown in Table 1. Samples A and B are practically identical. Any minor differences reflect processing errors and reproducibility limits. Sample C contains a higher amount of Nb and Ca dopant. The granulated powders have been produced by conventional solid state reaction technology, during which

a mixture of the oxide raw material precursors is prefired, milled and spray-dried. The introduction of the doping elements takes place during the milling of the prefired powders. The processing parameters have been kept identical for all three production batches.

For the sintering of the compacted specimens, three different sintering curves have been used, as indicated in Figure 1. They all correspond to a maximum temperature of sintering at 1380°C. The dwell time at the maximum temperature of sintering is 0, 4,5 and 9 hours for curves I, II and III, respectively. The heating and cooling rates have been identical. The sintering atmosphere has been 100% oxygen until one hour before the starting of the cooling stage, where it shifts to the appropriate equilibrium partial pressure of oxygen [1] that follows the samples during the entire cooling stage.

Tab. 1. Basic composition and dopant content of the three different granulated powders employed in the experiments

Basic Elements	Granulate A	Granulate B	Granulate C
Fe ₂ O ₃ (wt.%)	69,93	70,03	70,03
Mn/Zn ratio	1,1	1,1	1,1
Dopant			
CaO (wt.%)	0,014	0,010	0,017
SiO ₂	0,012	0,009	0,015
Nb ₂ O ₅	0,007	0,007	0,013
Bi ₂ O ₃	0,024	0,025	0,025
MoO ₃	0,042	0,040	0,040

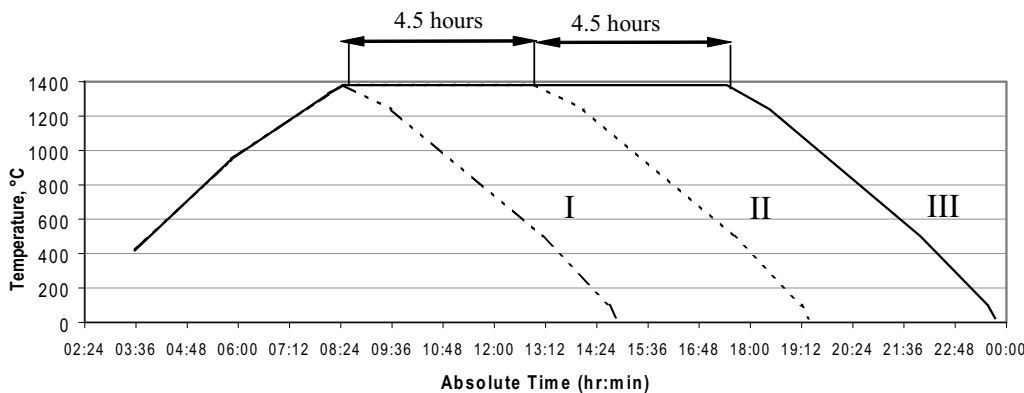


Fig. 1. Temperature profile of the three sintering schedules employed during the experiments

Tab. 2. Basic magnetic, electrical and structural properties of compacted specimens from granulates A, B and C after being sintered with sintering schedules 1, 2 and 3

Sintering schedule (Fig.1)	1			2			3		
	A	B	C	A	B	C	A	B	C
Granulate (Table 1)									
Final density (g cm ⁻³)	4,86	4,86	4,83	4,95	4,95	4,96	5,01	5,01	5,00
Initial Permeability μ_i 25°C 0,1mT, 10kHz	6040	6354	4396	9381	10099	7394	10145	10779	8088
Initial Permeability μ_i 25°C 0,1mT, 500kHz	3407	2367	4499	3530	2760	4766	2636	2337	2301
Losses, tan d/ μ_i 25°C 0,1mT, 30kHz [$\times 10^{-6}$]	6,2	10,6	1,9	2,5	3,3	1,7	3,1	3,5	3,4
Losses, tan d/ μ_i 25°C 0,1mT, 100kHz [$\times 10^{-6}$]	21,3	37,3	5,9	15,0	18,0	10,6	18,5	19,3	18,6
Specific Resistivity at 25°C, 10kHz (Ohm mm)	95	61	653	315	253	951	220	171	270

The resistivity was measured with a FLUKE 189 True RMS Multimeter on half toroids cross sectional area of which is coated with silver paste. The specific resistivity was

calculated by using the formula:

$$\rho = \frac{R \cdot A_e}{l_e} \quad (1)$$

where: A_e is the effective area and l_e the effective length of the half toroidal specimen.

The microscopic investigations are performed on polished and chemically etched surfaces of cross sections of the specimens, with an Aristomet optical microscope. The magnetic measurements are performed with an impedance-gain analyzer (HP4284A) equipped with oscilloscope, power amplifier and frequency generator, on toroids wound with copper wire to form inductors.

Results

The final density, basic magnetic properties and specific resistivity results are shown in Table 2.

As shown, the 10 kHz initial permeability of a particular composition increases as the dwell time at top temperature increases. In addition, within the same sintering schedule, specimen C gives constantly the lower permeability. The stability of the permeability as expressed by the 500 kHz initial permeability, in general follows Snoek's law [2]; the higher the initial permeability, the lower the frequency stability.

Among the three compositions, C is the one with the highest specific resistivity. However, when comparing the specific resistivity values of one composition in the three sintering schedules, it can be seen that the resistivity passes through a maximum at schedule 2. In Figure 2 the specific resistivity and the 10 kHz

are shown as a function of the maximum temperature of sintering dwell time for samples of composition C, accompanied with images of the obtained microstructures. Analogous results for samples of composition A are shown in Figure 3.

Discussion

The increase of the initial magnetic permeability as a function of the dwell time can be explained by the simple form of the non-magnetic grain boundary model, as described in literature [3]. It has been proposed that the effective permeability μ_e of a polycrystalline system consisting of grains with an average diameter D and permeability μ_i , surrounded by non-magnetic grain boundaries with thickness δ is given by the relation:

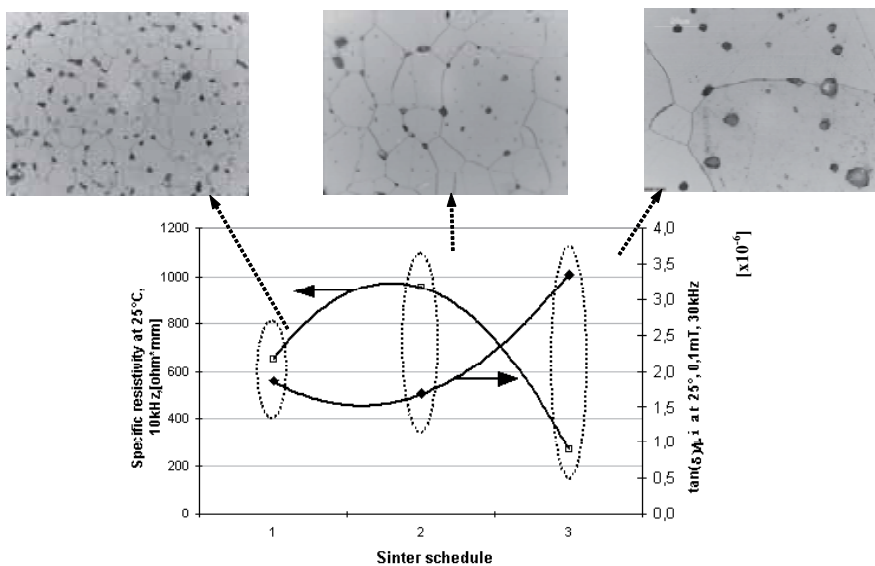


Fig. 2. Specific resistivity, losses and microstructures as a function of the maximum temperature of sintering dwell time for specimens of composition C

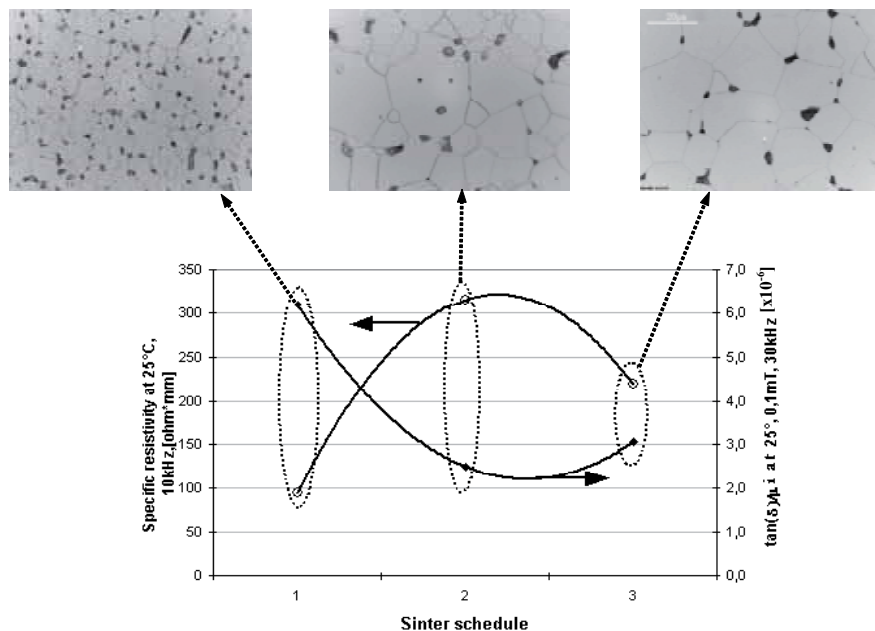


Fig. 3. Specific resistivity, losses and microstructures as a function of the maximum temperature of sintering dwell time for specimens of composition A

$$\mu_e = \frac{\mu_i D}{\mu_i \delta + D} \quad (2)$$

Equation (2) predicts, at all other parameters constant, an increase of the effective permeability μ_e with increasing grain size D .

Equation (2) has been modified in [4] where the grains are assumed to be surrounded by less magnetic grain boundary layers with permeability $\mu_{i,GB}$, that is inversely proportional to the so-called grain boundary resistivity (ρ_{GB}) as described in the formula:

$$\mu_e = \frac{(D + \delta)\mu_i\mu_{i,GB}}{\mu_i\delta + D[\mu_{i,GB} = f(1/\rho_{GB})]} \quad (3)$$

Subsequently, the lower initial permeability of specimens of composition C can be explained, since the higher amount

of dopants (e.g. CaO, Nb₂O₅) is considered to lead either to a thicker grain boundary or to a larger grain boundary resistivity and through this to a lower grain boundary permeability $\mu_{i,GB}$.

The low frequency specific resistivity as a function of the dwell time shows an unexpected behavior and passes through a maximum. As has been described earlier in literature in relation to frequency dispersion models [5], the low frequency specific resistivity can be very well considered to represent the grain boundary resistivity ρ_{GB} .

It is believed that the obtained maximum is related to the dopant distribution in the microstructure and represents the situation where dopant diffusion and grain growth rates match each other. The final situation is then a microstructure having all dopants homogeneously distributed along the grain-boundaries. When dopant diffusion is not sufficiently fast then dopants may still exist at the interior of the grains at the vicinity of the grain boundaries. On the other hand, when sintering is prolonged dopant diffusion along the grain-boundaries proceeds further resulting to a situation where they are accumulated at the triple points. The situation is schematically shown in Figure 4.

The situations represented by stages A and C provide also pinning points that consist energy barriers and disturb the smoothness of the magnetization process, in particular when the latter occurs via domain wall movement mechanism. This is also the reason that the low frequency losses show a minimum at this point as shown in Figures 2,3 and

Table 2. The high frequency losses are also co-determined by the resonance frequency (residual losses) that in turn is a strong function of the permeability and therefore grain size. This is the reason that the minimum is not always very clear in this case.

As found in a previous publication [4], the situation shown in stage B and in particular the high grain boundary specific resistivity is beneficial for the frequency stability of the initial permeability, within the limits of the law of Snoek [2] that dictates a permeability drop around the resonance frequency f_r given by the relation:

$$f_g = \frac{0.1\gamma B_s}{\mu_{i,0}} \quad (4)$$

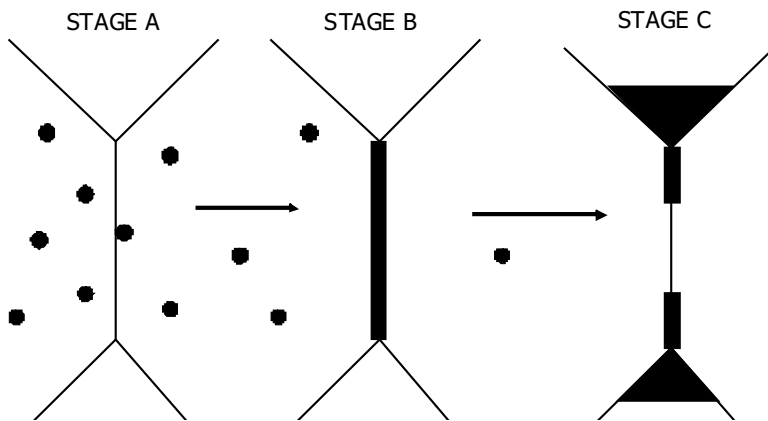


Fig. 4. Schematic diagram of the three distinguished dopant distribution situations during sintering: Stage A: when sintering stops before diffusion is completed, Stage B: when diffusion and sintering times are optimized, Stage 3: When sintering is prolonged after diffusion is completed

where: B_s is the saturation flux density, $\mu_{i,0}$ is the low frequency initial permeability and $\gamma \sim 0.22$ MHz m/A is the gyromagnetic ratio for an electron; i.e. the ratio of magnetic moment and torque.

For samples with identical initial permeabilities achieved through different strategies the highest frequency stability is exhibited by those with the highest d.c. (i.e. grain boundary) specific resistivity. Such a comparison is difficult to be made for the samples shown in Table 2, since they refer to different initial permeabilities. Nevertheless by comparing the basically identical samples A and B through all sintering schedules it can be seen that the high frequency permeability is always higher for the high specific resistivity sample.

From the industrial point of view it is very challenging to obtain frequency stable high-permeability ferrites at short sintering cycles. Based on the previous discussion this would require control of the dopant diffusion rate. Dopant diffusion in spinels occurs through a cation vacancy hopping mechanism and generally obeys the law of Fick:

$$J = D \frac{dC}{dx} \quad (5)$$

where: J is the flux, dC/dx the concentration gradient and D the diffusion coefficient, being a function of the cation vacancy concentration $D = f(V_c)$.

The initial dopant concentration and the cation vacancy concentration are thus important parameters in determining the dopant concentrations along the grain boundaries after a certain sintering time. The latter can be influenced either by the partial pressure of oxygen during sintering or by the introduction of dopants that generate cation vacancies. Work towards these directions is in progress in the laboratory.

Conclusions

The initial permeability in polycrystalline Mn-Zn-ferrites is basically determined by the average grain size since they both increase monotonically with increasing the dwell time at the maximum temperature of sintering.

In contradiction to that, the d.c. specific resistivity and the low frequency losses as a function of the dwell time at the maximum temperature of sintering pass through a maximum and minimum, respectively.

It is believed that this behaviour is related to the dopant distribution within the polycrystalline microstructure. A metastable situation might occur during sintering where the majority of the dopant concentration is accumulated along the grain boundaries. As found this point corresponds to the highest d.c. specific resistivity, lowest low frequency losses and maximum frequency stability.

Under conditions of slow dopant diffusion or prolonged sintering the previous situation may either not be achieved or disturbed and the optimum magnetic performance is not reached.

References

- [1] R. Morineau, M. Paulus, IEEE Trans. Magn., 5 (1975) 1312.
- [2] J.L. Snoek, Physica, 14 (1948) 207.
- [3] E.G. Visser, M.T. Johnson, J. Magn. Magn. Mater., 101 (1991) 143.
- [4] V.T. Zaspalis, J. Hanuszkiewicz, D. Holz, J. Appl. Phys., 103, (2008) 1.
- [5] C.G. Koops, Physical Review, 83 (1951) 121.

◆